Zero-THz Absorption Profiles in Glassy Solutions

High Frequency γ Process and its Characterisation

By Colin J. Reid and Myron W. Evans*

Chemistry Department, University College of Wales,
Aberystwyth, Dyfed SY23 1NE

It is established that in addition to the well-documented α and β losses in viscous fluids, there exists a third (γ) process at THz frequencies (far infrared, or submillimetre) which is necessary for the overall time-correlation function of the dipole moment to be well-behaved at short times. The β and γ peaks of the zero-THz loss profile survive in the glassy state as remnants of the microwave and Poley absorptions observable in the liquid at ambient temperature. In order to probe the glassy environment in non-dipolar solvents such as decalin, the behaviour of the following solutes is monitored : dichloromethane (10 % v/v); dibromomethane (3 % v/v); tetrahydrofuran (10 % v/v); toluene (20 % v/v); chloroform (10 % v/v); fluoro-, chloro-, and bromo-benzene (10 % v/v). Some of these solutes are used as probes also into the weakly dipolar glassy environment of o-terphenyl and (10 % pyridine+90 % toluene). The zero-THz absorption profiles of the solutes display a variety of behaviour above and below the glass transition temperature. For example, CH_2Cl_2+decalin has a very pronounced β process in the viscous liquid which is absent from CH_2Br_2 +decalin. The β process gradually disappears across the halogenobenzene+decalin series from fluoro- to bromo-.

The behaviour of the β and γ peaks for asymmetric, planar and intermediate solutes (*e.g.*, CH_2Cl_2, halogenobenzene and tetrahydrofuran) in dilute solution in glassy decalin, for example, confirm that they are different expressions of the same overall dynamical evolution. For CH_2Cl_2+decalin solid solutions the β peak moves very rapidly to high frequencies with increasing temperature. The associated Arrhenius activation enthalpy (ΔH_β) is thus extremely high compared with those of the larger molecules studied in the glass by Johari *et al.* and by Williams *et al.* There is a correspondingly dramatic shift in the THz(γ) peak to higher frequencies from its value in the liquid solution at 298 K to that in the glass at 107 K. In tetrahydrofuran+decalin glass ΔH_β is low and the shift in the γ peak much smaller. The same is true for the halogenobenzene+decalin glasses where present data for the β process are in excellent agreement with those of Johari *et al.*, where available.

A crude but tractable model capable of reproducing both β and γ processes of the glassy condition is that of itinerant libration.

It is now established [1] that the broad-band far infrared absorption observed in dipolar liquids is the high frequency part of a profile extending from zero to THz frequencies. This profile, which may be expressed in terms of dielectric loss [$\varepsilon''(\omega)$], or power absorption $\alpha(\omega)$, or Rayleigh depolarised light intensity [$\varepsilon''(\omega)/\omega$], is the Fourier transform into the frequency domain (ω) of an orientational time-correlation function $C(t)$. This profile, sketched on a log–log scale in fig. 1, is a *measure* of the rotational motions of the molecules in the condensed state of matter but is an *outcome* of rototranslational coupling, which must be an important consideration [2] in the development of a model for $C(t)$. This modelling may be accomplished by a matrix Mori expansion of the Liouville equation, [3] but to keep to a minimum the number of adjustable parameters, we seek in this paper an experimental situation where the molecular rotation may be treated in isolation of the centre of mass translation to a good approximation. This is the case for rigid dipolar molecules dissolved in non-dipolar or weakly dipolar glasses. [4] For $C(t)$ to be well-behaved it must follow that

the far infrared absorption in the glass is considered an integral part of the loss pro-file.[5]   In a viscous fluid we have established already that the latter consists of three interlinked loss bands designated as primary, secondary and tertiary with respect to the overall dynamical evolution.[6]   The tertiary process is one of libration, very fast compared with the others, and showing up as a THz (far infrared) loss ; the secondary (β) process is the influence of nearest neighbour cage fluctuations on the libration, creating a diffusion of the encaged molecule from one energy well into another.   This has been described by Johari et al.[7] and by Williams [4] as a remnant of the liquid-like rotational diffusion observed at ambient temperatures, the loss process first explained by Debye.   Only the β process continues to be observable in the glass, with in most cases an activation enthalpy similar to its value at ambient temperature.   The primary (α) process is one of bulk reorientation (inclusive of next nearest neighbours etc.), and is the slowest.   In the glass the cooperative motion becomes infinitely slow, and the α loss peak moves to zero frequency, leaving the β and far infrared (or γ) processes as a continuum profile to be linked analytically by a suitable simple model of the angular dynamics of individual molecules.   In this context it is important to realise that a Debye model for the β process, besides being too narrow in loss half-width, would not reproduce the γ process at all, but rather the unacceptable Debye plateau (seen before the resonance in fig. 1) in the power absorption coefficient $\alpha(\omega)$.   Inclusion of inertial effects in the Debye model still
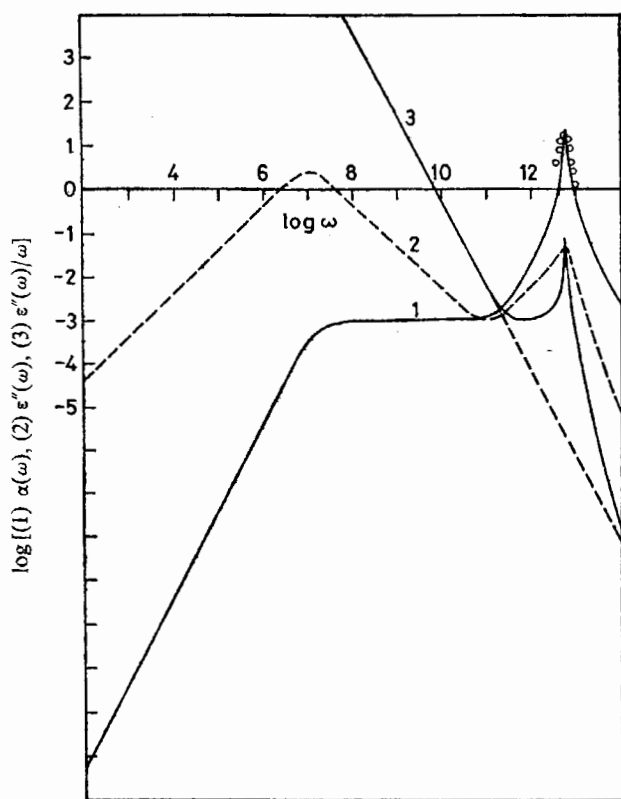

FIG. 1.—Schematic diagram of (1) $\alpha(\omega)$, (2) $\varepsilon''(\omega)$ and (3) $\varepsilon''(\omega)/\omega$ as a function of ω on a logarithmic scale for glassy substances, (β and γ processes only).

does not produce the γ peak, but merely a slow return to transparency at the high frequency end of the plateau. In this paper we produce linked β and γ processes using an itinerant libration formalism extended recently by Coffey *et al.*[8] to include the effect of its inertia on the torsional oscillation of a given molecule.

As the librational band represents the short-time details of the molecular torsional oscillation, data which encompass the whole zero-THz range are needed. Therefore, in this paper a number of solutions of rigid molecules in decalin have been studied at low temperatures (77-153 K) both in the 0.5-100 kHz region of the β loss process and in the 20-220 cm^{-1} region of the far infrared, where the γ process is discernible as the Poley absorption[1] shifted in the glass to higher frequencies. Among the systems studied, glasses of CH_2Cl_2 in decalin, toluene+pyridine and o-terphenyl are of especial interest for the following reasons. (i) CH_2Cl_2 is a small molecule whose inertial framework is nonetheless very asymmetric, so that its rotation in the glass might be strongly hindered. (ii) Extensive and accurate data exist for this molecule in the far infrared[9] and in related spectroscopic fields[10] such as depolarised Rayleigh and incoherent neutron scattering.

EXPERIMENTAL

The far infrared optical absorption coefficients [$\alpha(\omega) = \log_e(I_0/I)/d$, where d is the sample thickness and I and I_0 are transmitted and incident intensities] were measured with a Grubb–Parsons/N.P.L. mark III interferometer by Fourier transformation of the phase modulated signal reaching an IR50 Golay detector (Unicam). A cell, constructed to hold the sample at a constant low temperature (± 1 K) utilised a glass jacketted dewar vessel with a pair of clampable copper plates at the base of the cold finger. This attachment (Grubb–Parsons) fits via an O-ring seal into an evacuable chamber, at the exit stop of the interferometer. A rectangular groove (44 mm × 23 mm cross-section) allowed an assembly of two TPX windows and a poly(ethylene) spacer to be clamped together to form a vacuum-tight cell. Thermocouple wires passed through the spacer to form the junction within the sample just below the beam. A lowest temperature of about 107 K could be achieved using liquid N_2 as coolant while higher temperatures were attained using two 20 W elements (1 cm × 3 cm) attached symmetrically on the metal plate edges. Filling of the cell was effected *via* a port in the spacer just large enough to take a syringe needle, this being then heat sealed. As the beam passes only through the central part of this cell there is sufficient liquid in the whole cell to prevent the appearance of a contraction gap in the sample upon cooling. The TPX windows used were 1.5 mm thick and consequently slightly flexible, especially after contact with samples. This thickness was a compromise between path-length inaccuracy and window attenuation, but still leaves some uncertainty in the absolute intensities of the spectra. The use of various path-lengths between 0.6 and 3.5 mm (8 mm for pure decalin) allows us to quote intensities to within ± 10 %. A more rigid material such as quartz was unusable because of possible breakage under the stresses present on cooling and its high frequency attenuation (above 100 cm^{-1}). Spectra of glass samples were obtained normally by ratioing the transform of the sample (I) over that of the decalin under identical conditions (I_0), except for weak solutes where a proportion of solvent spectrum must be added : this method gives automatic correction for solvent absorption. The pure decalin spectrum was obtained by ratioing transforms of thick sample to thin sample, thereby avoiding reflection losses. The ambient temperature spectra were recorded using a standard VC01 variable pathlength cell with TPX windows.

The dielectric spectra were recorded using a similar holder. The cell assembly consists of two aluminium plate electrodes separated by a 1 mm Teflon spacer. To one side of one electrode was a " non-active " cell joined to the main cell *via* drilled holes, and acting as a reservoir and a housing for the thermocouple. The advantage of this section is that the spacer, being made of polyethylene (PE), allows filling and sealing of the whole cell, as above. The use of a single section, *i.e.*, two electrodes and a spacer could not have included PE for the latter as it readily absorbs solute and would then contribute dielectric losses and so could not have utilised the heat-sealing property of PE.

RESULTS

In table 1 we summarise our available THz data in liquid decalin at ambient temperature and introduce a factor $I^*\bar{v}_{max}^2$, the product of reduced inertia (I^*) and the square of the far infrared frequency of maximum absorption ($\bar{v}_{max}^2$). This is a measure of the mean square torque on the solute molecule (the probe). The data in table 1 fall into groups according to the shape of the solute molecule as indicated by $I^*\bar{v}_{max}^2$. However, to some extent their peak positions tend to be independent of solvent so the molecules are experiencing a nearly spherical force field. Table 2 summarises the situation in the viscous liquid and glass for various types of α, β and γ processes in decalin solvent, which is ideal as a supercoolable medium, since its dielectric loss is negligible and its far infrared absorption small compared with those of typical dipolar solutes such as CH_2Cl_2. All spectra are corrected for solvent absorption assuming throughout that the solvent contribution is subtractable, *i.e.*, the presence
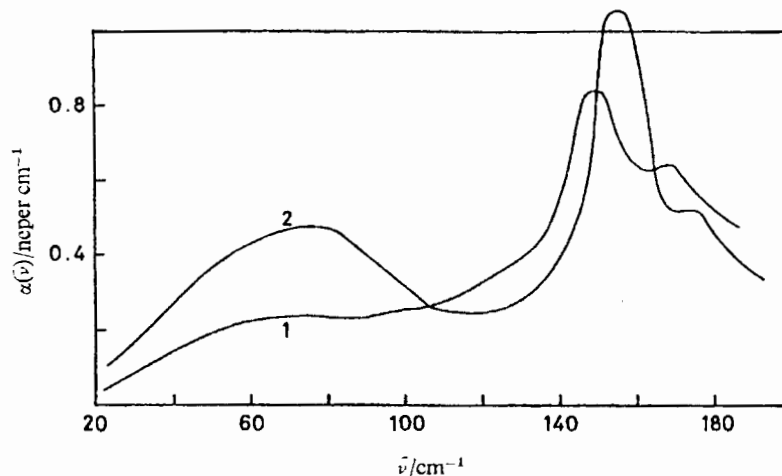

FIG. 2.—Far infrared absorption of decalin at (1) 298 and (2) 107 K.

of probe molecules does not significantly affect the solvent absorption. The far infrared collision induced band of decalin solvent is illustrated in fig. 2 for the liquid at 298 K and for the glass at 107 K. The absorption peaking at 70 cm^{-1} at 298 K narrows at the lower temperature. Solutions in decalin, even when dilute, tend to crystallise, but it was found possible with the cell arrangements used to cool a 10 % v/v fraction solution rapidly through the region of instability around 180 K (the melting point of decalin) to the glass transition temperature (T_g) at $\approx$ 130 K with negligible component separation. Three types of process are discernible; (i) " prominent ", where β is well separated from α in the viscous liquid; (ii) " shoulder "; and (iii) " absent ". The half-widths observed are $\approx$ 3-4 decades, so that the range studied may just accommodate a single peak at a given temperature.

The temperature variation at three frequencies of log (loss tangent) is displayed in fig. 3 and the permittivity at 1 kHz in fig. 4 for these decalin solutions. The permittivity in particular betrays the onset of a glass → viscous liquid transition.

In table 3 the main features of the far infrared bands in decalin at 107 K are recorded, together with the fractional change in the factor $I^*\bar{v}_{max}^2$. This indicates to what extent the mean square torque has increased in the glass for a given probe.

TABLE 1.—PROBE MOLECULES IN DECALIN AT 298 K

solute[a]	moments of inertia[b] /10^{-45} kg m^2		reduced inertia (I^*)	$\bar{v}_{max}$ f.i.r. peak (298 K)/cm^{-1}	$I^*\bar{v}_{max}^2$	type
bromobenzene ($z = 1.63$ Å)	9.67 8.2 (1.45)	C_6	4.43	24	2551	planar 6 ring
chlorobenzene ($z = 0.98$ Å)	6.83 5.52 (1.45)	C_6	3.05	33	3321	
fluorobenzene ($z = 0.44$ Å)	4.71 3.24 (1.45)	C_6	1.92	39	2920	
toluene ($z = 0.46$ Å)	4.77 3.25 (1.49)	C_6	1.92	60 (shoulder)	6912	planar 6 ring bulky side group
nitrobenzene ($z = 1.22$ Å)	8.98 6.90 (2.1)	C_6	3.90	40	6240	
THF	2.29 1.32 0.91	C_5	0.82	46±6	1746	" semi rigid " 5 ring
furan	1.88 0.94 1.1		0.6	51	1560	planar 5 ring
thiazole	2.58 1.54 0.97		0.83	45	1680	
CH$_2$Cl$_2$ (approx. prolate symmetric top)	0.26 2.65 (2.8)		0.23	54	670	small ellipsoids
chloroform (oblate symmetric top)	2.53 2.53 (5.0)		1.26	28	992	
CH$_3$CN (CCl$_4$ solvent)	0.875 0.875 (0.05)		0.437	73	2328	almost linear
SCl$_2$	4.4 0.26 (3.82)		0.24	50	612	small ellipsoids
CH$_2$Br$_2$	0.32 6.79 (6.9)		0.30	54	875	

[a] z is displacement of mass centre from C_6-ring centre.   [b] Moments of inertia are estimated from bond length data, bracketted value being that along dipole axis.

TABLE 2.—α, β, γ SPECTRAL DATA

solution in decalin	β peak type	β temperature/K (when centred at:) 500 Hz	β temperature/K 50 kHz	β mean value of ΔH_β /kJ mol⁻¹	β ε''_{max} at 10 kHz	β half width at 10 kHz (decades)	α peak temp./K (when centred at 10 kHz)	α ε''_{max}	f.i.r. peak position ($\bar{\nu}$/cm⁻¹) when at 107 K	f.i.r. when at 2981 K
10 % CH₂Cl₂	prominent	110	114	95	0.052	3.2	—	—	113	54
5 % CH₂Cl₂	prominent	110	114	95	0.021	3.8	—	—	100	53
3 % CH₂Br₂	absent	—	—	—	—	—	146	0.019	105	54
10 % PhF	prominent	—	77	12	0.045	4	146	0.026	57	39
10 % PhCl	shoulder	113	132	27	(0.022)	4	(142)	(0.08)	53	33
10 % PhBr	absent	—	—	—	—	—	144	0.2	42	24
10 % THF	prominent (not measurable)	—	77	10	0.08	—	140	0.035	80	46
20 % toluene	faint shoulder	106	122	30	0.004	—	141	0.0096	90	60
10 % chloroform	shoulder	102	125	24	0.022	4	141 (half widths ≈ 3.2)	0.004	51	28

Brackets denote uncertainty arising from poor peak resolution.

For the halogenobenzenes the factor $I^*\bar{v}_{max}^2$ is large initially and increases by 100–200 %. The fluorobenzene is less hindered, which is commensurate with the observed low frequency " permittivity decrement " of $\Delta\varepsilon = (\varepsilon_0 - \varepsilon')/(\varepsilon_0 - \varepsilon_\infty) = 0.55$, i.e., this molecule can still relax easily in the glass.* Toluene becomes slightly hindered in the glass and so still possesses a β relaxation. Possibly the CH_3 rotation causes a large fluctuation of the potential barrier, rototranslationwise. To a lesser extent this occurs for tetrahydrofuran. In these cases it is probable that a mechanism of hexad rotation predominates. By using the measured ΔH_β values (fig. 5) and the moment of inertia for this C_n-axis we can estimate the THz libration frequency using the Brot–Darmon harmonic oscillation model.[12] This produces delta frequencies recorded in column 3 of table 3. Denoting this frequency by $\bar{v}_{harm}$, they are high compared with the experimental value in chlorobenzene and fluorobenzene, but too low for tetrahydrofuran (however ΔH_β here is more uncertain). Theoretically
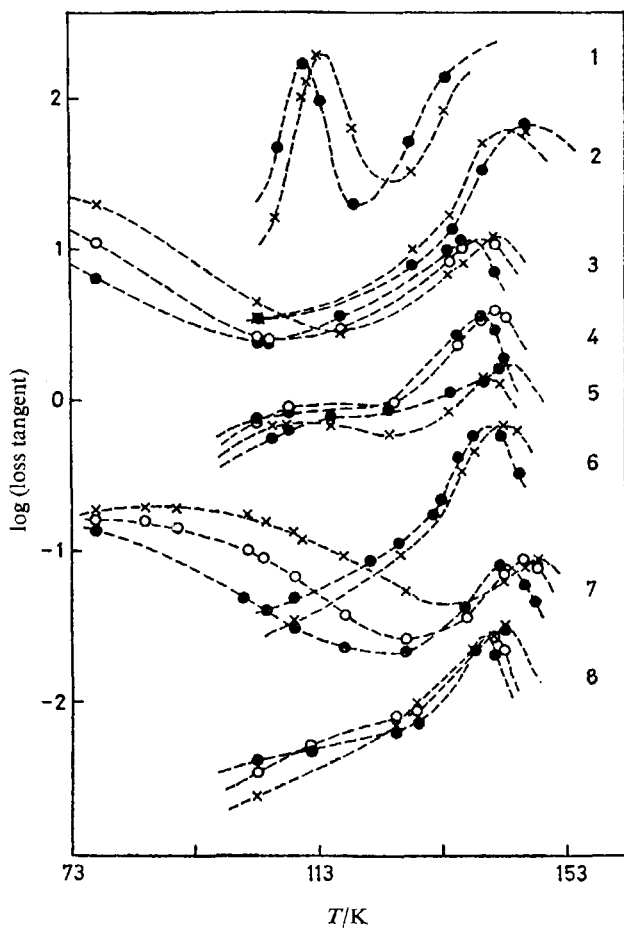
FIG. 3.—Loss tangents for decalin solutions at : ●, 50 kHz ; ○, 5 kHz ; ×, 500 Hz ; (1) 10 % v/v CH_2Cl_2 (raised by 4 decades) ; (2) 3 % CH_2Br_2 (raised by 4 decades) ; (3) 10 % tetrahydrofuran (raised by 3 decades) ; (4) 20 % toluene (raised by 2 decades) ; (5) 10 % chloroform (raised by 2 decades) ; (6) 10 % bromobenzene (raised by 1 decade) ; (7) 10 % fluorobenzene (raised by 1 decade) ; (8) 10 % chlorobenzene.

* Here ε' is measured at 1 kHz, ε_∞ is the value for decalin, and ε_0 is extrapolated from fig. 4.

of course, the β peak should move to low frequencies (from the microwave) in the glass and the γ peak to higher frequencies from those observed in the liquid. This is observed in every case monitored in this paper. The large $\Delta I^* v_{max}^2$ in THF may be explained in that initially at 298 K this probe rotates easily within a decalin cage whose enclosure is larger than THF. As the sample cools the enclosure becomes the same size. There is still appreciable rotation so one would predict that in a glass of smaller solvent molecules the far infrared peak will be higher. A similar prediction could be made for CH_2Cl_2. Although the $\Delta I^* v_{max}^2$ is large and the permittivity decrement implies that the glass is rigid, we know that at this temperature the β process peak has only just passed the monitoring frequency so that presumably the cage is just beginning to close in. This is supported by the fact that the Brot–Darmon harmonic oscillator predicts higher frequencies using ΔH_β of $\approx$ 100 kJ mol^{-1}.

TABLE 3.—PROBE MOLECULES IN GLASSY DECALIN (107 K)

solute in decalin	f.i.r. peak /cm^{-1}	harmonic model,[12] $\bar{v}_{harm}$/cm^{-1}	$\Delta I^* \bar{v}_{max}^2$	fraction permittivity decrement[a] (500 Hz)
10 % bromobenzene	42	—	3.06	0.9
10 % chlorobenzene	53	58 ($n = 6$)	2.58	0.82
10 % fluorobenzene	57	60 ($n = 6$)	2.13	0.55
20 % toluene	90	77 ($n = 6$)	2.25	0.65
10 % THF	80	50 ($n = 5$)	3.02	0.6
5 % furan	80	—	(2.46)	0.55
10 % CH_2Cl_2	113	—	4.38	0.8
10 % chloroform	51	45 ($n = 3$)	3.31	0.6
10 % SCl_2	64	—	1.64	0.55
3 % CH_2Br_2	105	—	3.78	0.72

[a] This is defined as $(\varepsilon_0 - \varepsilon')/(\varepsilon_0 - \varepsilon_\infty)$, (see text).

Table 4 compares some far infrared and dielectric data for two other weakly dipolar types of glass: o-terphenyl, a large planar molecule, and a mixture of pyridine and toluene. Decalin, being non-dipolar, is a poor solvent for intensely dipolar probes such as CH_3CN and pyridine at low temperature. Conversely, pyridine + toluene is an intensely absorbing solvent so that weakly dipolar probes are not suitable. CH_2Cl_2 and fluorobenzene have been compared in all three glasses. In o-terphenyl, fluorobenzene has a β peak but the β peak of CH_2Cl_2 was not observed and is presumed present at higher frequency. The latter far infrared (γ) peak is also relatively low at 103 cm^{-1}, implying less hindrance than in decalin. In pyridine + toluene there are no appreciable β relaxations in the glass (except that due to the solvent). The γ process has shifted a very long way to *higher* frequency in the far infrared for the CH_2Cl_2 solution compared with the position in the liquid at 298 K (fig. 6).

It is informative to compare the temperature shifts in the far infrared for dichloromethane in decalin and pyridine + toluene glasses. In decalin the shift was 6 cm^{-1} between 127 and 107 K, a change of 1 cm^{-1} per 3.3 K. This is mirrored in the overall shift from 54 to 113 cm^{-1} between 298 and 107 K (*i.e.*, 1 cm^{-1} in 3.3 K). The shift remains linear in the glass. In pyridine + toluene a shift of 3 cm^{-1} in 17 K is measured
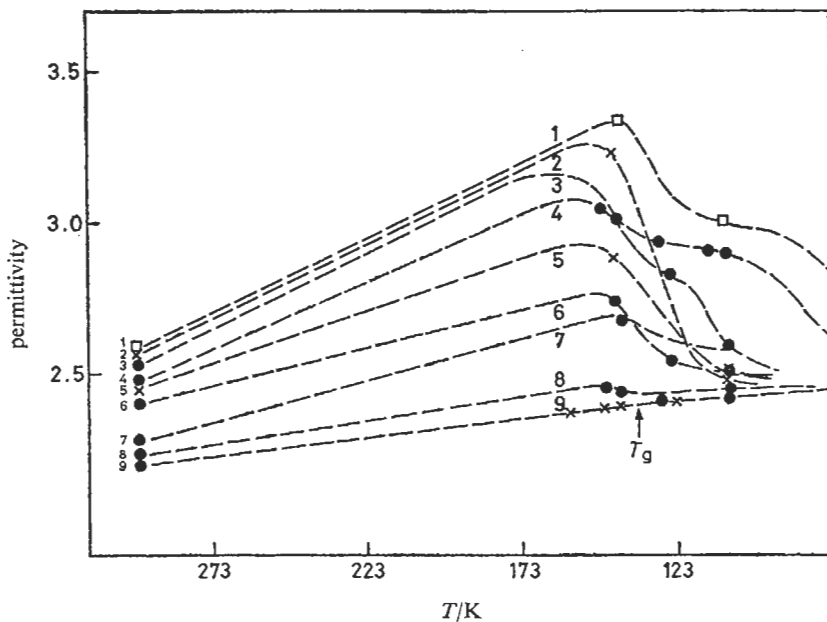
FIG. 4.—Permittivity variation with temperature at 1 kHz for some decalin solutions: (1) 10 % v/v tetrahydrofuran; (2) 10 % bromobenzene; (3) 10 % dichloromethane; (4) 10 % fluorobenzene; (5) 10 % chlorobenzene; (6) 10 % chloroform; (7) 10 % sulphur dichloride; (8) 20 % toluene; (9) pure decalin.
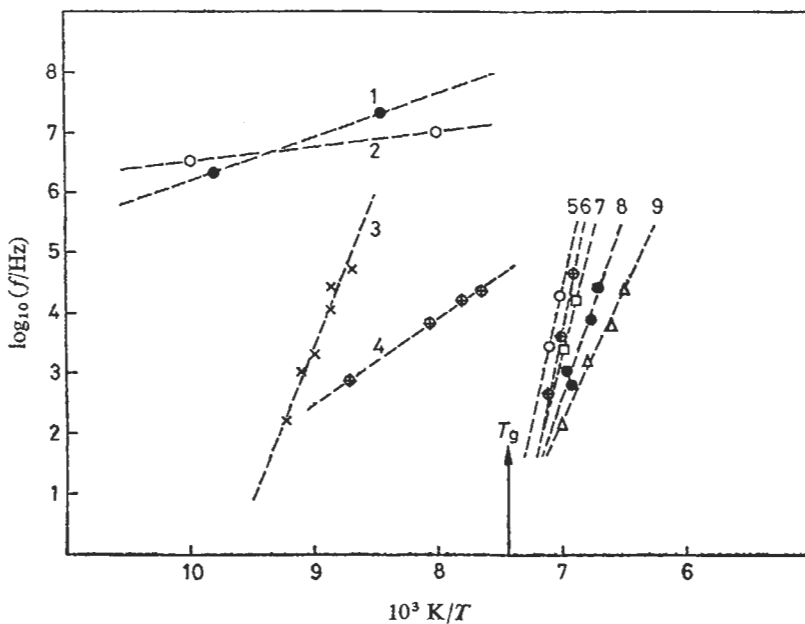

FIG. 5.—Activation energy plots for processes (α, β) observed in decalin (10 % v/v solutions). (1) Fluorobenzene (β); (2) tetrahydrofuran (β); (3) dichloromethane (β); (4) chlorobenzene (β); (5) tetrahydrofuran (α); (6) chlorobenzene (α); (7) bromobenzene (α); (8) fluorobenzene (α); (9) 1-bromo-3-methylbutane (α).

in the low temperature glass (1 cm^{-1} in 3.5 K), but the overall shift is from 62 to 140 cm^{-1} in 193 K, a massive change taking place at an average rate of 1 cm^{-1} in 2.2 K. In this glass, therefore, the rate of shift has slowed, which indicates that CH$_2$Cl$_2$ becomes very highly hindered just below the glass transition (T_g), and further hindrance occurs only very slowly. The linear shift in decalin indicates the continued existence of the β process.

TABLE 4.—F.I.R. PEAK COMPARISONS FOR 3 ORGANIC GLASSES (107 K)

solute	decalin			o-terphenyl			10/90 pyridine + toluene		
	f.i.r. peak/cm^{-1}	$\Delta I^* \bar{v}_{max}^2$	$\Delta \varepsilon$	f.i.r. peak/cm^{-1}	$\Delta I \bar{v}_{max}^2$	$\Delta \varepsilon$	f.i.r. peak/cm^{-1}	$\Delta I \bar{v}_{max}^2$	$\Delta \varepsilon$
10 % CH$_2$Cl$_2$	113	4.38	0.8	103	3.6	(0.8)	140	5.8	0.85
10 % fluorobenzene	57	2.13	0.55	56	2.0	0.6	70	3.0	0.88
3 % CH$_3$CN	—	—	—	90	1.52	—	120	2.7	0.85
10 % pyridine	—	—	—	—	2.05	0.6	76	2.85	0.85
5 % nitrobenzene	—	—	—	—	—	—	48	1.43	0.9
3 % benzonitrile	—	—	—	—	—	—	74	—	0.9

$\Delta \varepsilon = (\varepsilon_0 - \varepsilon')/(\varepsilon_0 - \varepsilon_\infty)$ (see text)
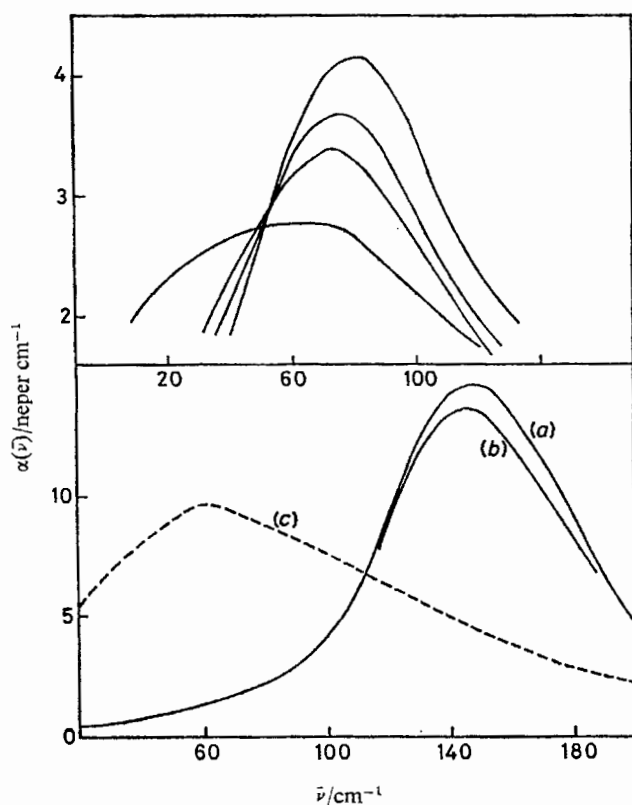

FIG. 6.—Upper : variation with temperature of the far infrared absorption of decalin + tetrahydrofuran (3 % v/v of the latter). Top to bottom 110, 128, 139, 298 K. (Corrected for decalin absorption). Lower : the same for 12 % v/v CH$_2$Cl$_2$ in pyridine + toluene solvent mixture (corrected for) (a) 105, (b) 121, (c) 298 K.

DISCUSSION

We confine our quantitative discussion in this paper to the glassy state where only the β and γ processes survive. Our aim is to show that the β process should not be modelled without its high frequency far infrared adjunct (the γ band). Therefore, we use the simplest physical model of the glassy state having the necessary minimum capability of reproducing the gross features observed experimentally. Such features are typified in CH_2Cl_2 + decalin glass, where the β peak sweeps across two decades of frequency in only 4 K, implying $\Delta H_\beta = 100 \pm 15$ kJ mol^{-1}. The γ peak also shifts dramatically in frequency. The root mean square angular velocity for a freely rotating ensemble of gaseous CH_2Cl_2 is 21.2 cm^{-1}, so that the change in the far infrared peak frequency $\bar{\nu}_{max}$ produced by a glassy environment is commensurate with that produced by condensing the infinitely dilute gas into the liquid at 298 K. (At the same time the β part of the total loss moves from 180 GHz at 298 K to 5 kHz in the glass at 111 K.) Much smaller shifts in $\bar{\nu}_{max}$ are observed [11] by use of k bars of external pressure on liquids such as C_6H_5Cl and CS_2.

We assume, therefore, that the rotational dynamics in the dilute glassy solution may be interpreted by means of the autocorrelated part of $C(t)$, and that the dipole and reaction field are parallel at all times. The dynamical evolution is described classically then by means of the Liouville equation, which may be written according to Mori [13] as

$$\dot{A}(t) = i\,\Omega_A A(t) - \int_0^t d\tau\, \phi_A(t-\tau)A(\tau) + F_A(t). \tag{1}$$

Here $A(t)$ denotes an $n \times l$ column vector with elements $A_j(t)$, which are linearly independent, real valued (implicitly), time-dependent dynamical variables of the glassy solute molecules. $i\Omega_A$ is a resonance operator, which is null when cooperative motions are not accounted for. The matrix kernel ϕ_A is a memory function (the effective liouvillian) and $F_A(t)$ is the Mori-projected random torque or force. Using a suitable approximation to eqn (1) we attempt in this paper to reproduce the main features of the β and γ processes with the minimum number (one) of adjustable parameters. A continuous loss profile is needed covering about nine decades of frequency peaking at kHz and THz frequencies.

In approximating eqn (1) for $C(t)$ it is assumed that superimposed on the process of torsional oscillation giving rise to the THz γ peak is a very much slower diffusion (the β process) through large angles, which is made possible by the irregular packing of solvent molecules around those of the solute in the glassy state. This situation may be modelled very crudely as follows. The direction of the solute dipole vector μ is specified by an angle $\theta(t)$ relative to the measuring field, while a point making an angle $\psi(t)$ relative to the same field vector is taken in the cage of nearest neighbours, which is assumed rigid, of moment of inertia I_1. The β process is then one of planar rotational diffusion, through infinitesimally small increments, of this rigid cage, carrying the inner dipole along with it. This dipole is also librating at a frequency ω_0, harmonically bound to the cage. The friction between the cage and its surroundings is

$$\beta_1 = kT\tau_D/I_1 \tag{2}$$

while that between the solute and solvent cage is β_2. Here $1/\tau_D$ is the angular frequency of the β peak, ω_0 that of the γ peak. This model fulfils the minimum requirements of producing (fig. 1 and 7) a continuous zero-THz loss profile with

β and γ features of finite width at half peak-height. Both the angular velocity and orientational autocorrelation functions are well behaved in that they have zero slope as $t \to 0$. This is a necessary, but not sufficient, condition for the appearance of the γ peak in the far infrared. A further condition, that the angular velocity a.c.f. be oscillatory, is necessary and is fulfilled by the resonance centred at ω_0. Both calculation and computer simulation have shown this to be true for the itinerant librator model used here.

The limitations of the model are as follows. (1) The β process is observed to be actually much broader than the profile produced analytically (fig. 7). This stems from taking a model of simple rotational diffusion for the cage reorientation. (2) The concept of planar reorientation of a rigid cage of neighbours in the glassy state is, of course, artificial, but otherwise the mathematics become intractable very quickly.
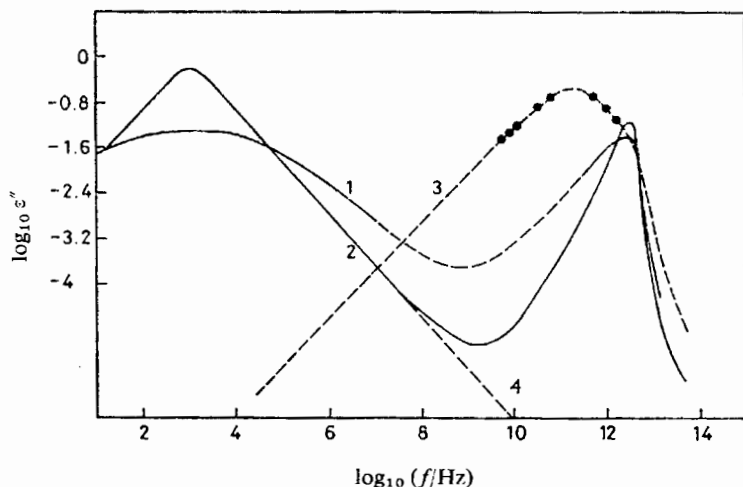

FIG. 7.—Complete spectrum of 10 % v/v CH_2Cl_2 + decalin : (1) experimental curve at 110 K (extra-polated to the microwave region by - - -); (2) analytical model curve at 110 K (for parameters see table 5); (3) experimental points ($\bullet$) on the analytical curve at 298 K; (4) Debye process (no description of γ peak possible).

Unfortunately, computer simulations [14] are not useful for linking the β and γ (and α in the viscous liquid) processes because of the long time scales involved. However, a recent simulation [15] of nitrogen in the glassy state has produced angular velocity autocorrelation functions which were highly oscillatory up to 1 ps, suggesting the presence of THz resonance (not observable dielectrically in N_2 of course, because there is no dipole). (3) It would not be possible to produce a further α process with a null resonance operator, $i\Omega_A$, as in this model. Therefore, it is not applicable to the viscous fluid, where in CH_2Cl_2 + decalin the α, β and γ processes are all fully resolved.

Defining Ω_0 as $(I_2/I_1)\omega_0$, the dynamical system evolves according to eqn (1) with:

$$A(t) = \begin{bmatrix} \theta(t) \\ \dot{\psi}(t) \end{bmatrix}; \qquad \phi_A = \left[\begin{array}{c|c} \beta_2\delta(t)+\omega_0^2 & -\omega_0^2 \\ \hline -\Omega_0^2 & \beta_1\delta(t)+\Omega_0^2 \end{array}\right]; \qquad F_A = \begin{bmatrix} W_2 \\ W_1 \end{bmatrix}$$

and a null resonance operator. Here W_2 and W_1 are Wiener processes.[8] This is a special case of the system developed by Damle et al.[16] for translational itinerant oscillation in space for incoherent neutron scattering. $\delta(t)$ is the Dirac delta function.

Varying β_2 has the effect of broadening or narrowing the γ curve.   Fig. 8 illustrates the γ curve in CH_2Cl_2 + decalin together with theoretical curves for values of β_2 in THz.   Values of ω_0, β_1 and β_2 are listed in table 5, and some correlation functions $-\ddot{C}(t)$ in fig. 9.   The function $-\ddot{C}(t)$ is the direct Fourier transform of $\alpha(\omega)$, and is similar numerically to the angular velocity autocorrelation function $\langle \dot{\theta}(t)\dot{\theta}(0)\rangle$.   We have $C(t) = \langle \cos\theta(t) \cos\theta(0)\rangle$. $\langle \dot{\theta}(t)\dot{\theta}(0)\rangle$ is oscillatory since such a result is obtained also in a simulation of N_2 glass, so that it is consistent to regard the γ process as reflecting predominantly the torsional oscillation of the solute dipole moment.
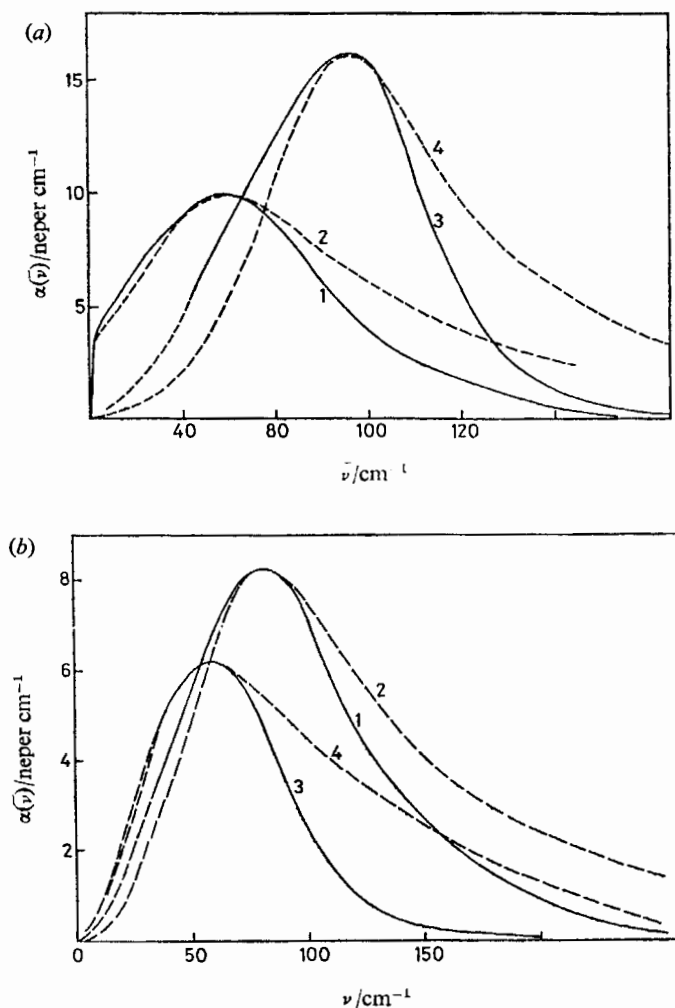

FIG. 8.—(a) THz part of the total absorption on 10 % v/v CH_2Cl_2 + decalin; experimental and analytical curves: (1) spectrum at 300 K (half scale); (2) analytical curve at 300 K, parameters as in table 5; (3) spectrum at 110 K; (4) analytical curve at 110 K or 113 K, parameters as in table 5. [Theoretical and exptl. curves are normalised.]   (b) Analytic and experimental THz curves for tetrahydrofuran (6 % v/v) and fluorobenzene (10 % v/v) in decalin solution: (1) tetrahydrofuran + decalin experimental curve at 110 K; (2) analytical curve (table 5); (3) PhF + decalin experimental curve at 110 K (double scale); (4) analytical curve, $\beta_2 = 20$ THz (normalised).

TABLE 5.—PARAMETERS FOR ITINERANT LIBRATION

sample[a]	I_2 /10^{-39} g cm² [b]	T/K	ω_0(exp) /10^{12} s⁻¹	f_{Debye} /10^9 s⁻¹	ϵ_0	ϵ_∞	ω_0 /10^{12} s⁻¹	I_1 /10^{-39} g cm²	β_1 /10^{12} s⁻¹	β_2 /10^{12} s⁻¹
CH₂Cl₂+decalin	2.37	300	10.7 (58 cm⁻¹)	1.8×10^{11}	2.56	2.19	9.3	2.37	30.9	20
		113	20.1 (111 cm⁻¹)	2.0×10^4	~ 3.40[d]	~ 2.41	20.7	23.7	10.5×10^6	20
		110	20.8 (112 cm⁻¹)	1.0×10^3	~ 3.40	~ 2.41	20.8	23.7	2.04×10^8	20
PhF+decalin	20.3	300	8.76 (46 cm⁻¹)	$\sim 2.0 \times 10^{10}$	2.40	2.20				
		110	10.7 (58 cm⁻¹)	$\sim 5.0 \times 10^6$	~ 3.30	~ 2.41	10.7	203	2.38×10^4	20
		77	—	$\sim 5.0 \times 10^4$	~ 3.46	~ 2.44				
THF+decalin[c]	8	300	11.1 (60 cm⁻¹)	—	2.58	2.19				
		110	15.45 (82 cm⁻¹)	$\sim 10^8$	~ 3.50	~ 2.40	15.45	80.0	6040	20
		77	—	$\sim 10^6$	—	—				

[a] All concentrations 10 % v/v when made up at 293 K; [b] reduced inertia $I_2 = I_x I_y/(I_x+I_y)$; [c] THF has pseudorotatory (proper) modes which may complicate the spectra at 300 K; [d] $\sim$ indicates the value is derived by extrapolation. Maximum estimated uncertainly, ± 10 %.
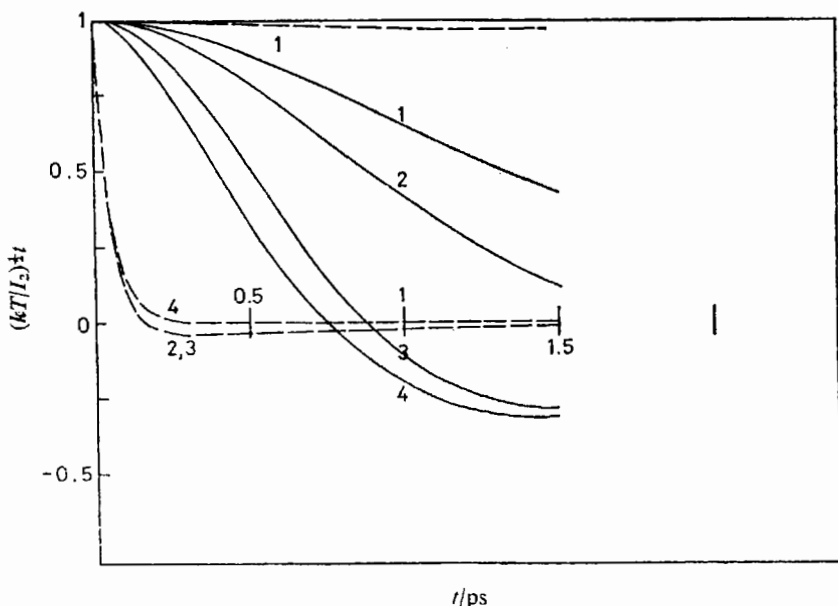
FIG. 9.—Correlation functions for CH_2Cl_2 + decalin systems. (a) (—) (1) Liquid solution, orientational autocorrelation function, $\langle \cos \theta(t) \cos \theta(0) \rangle$; (2) normalised angular velocity autocorrelation function, $\langle \dot{\theta}(t)\dot{\theta}(0)\rangle/\langle \dot{\theta}(0)\dot{\theta}(0)\rangle$; (3) normalised rotational velocity a.c.f. $\langle (d/dt) \cos \theta(t)[(d/dt) \cos \theta(t)]_{t=0} \rangle$; (4) normalised torque autocorrelation function $\langle \ddot{\theta}(t)\ddot{\theta}(0)\rangle\langle \ddot{\theta}(0)\ddot{\theta}(0)\rangle$. (b) (- - -) (1) to (4). As for (a), but in the glass.

Whatever the molecular dynamical explanation adopted it has been the main purpose of this paper to emphasise that the loss profile in glassy solids consists of two well separated peaks, one of which, the γ process, having the characteristics of a Poley absorption. The existence of the process is necessary on fundamental grounds and is due to short time torsional oscillations of the solute dipole. The behaviour of these peaks for asymmetric, planar and pseudo-symmetric solutes in different glasses confirms they are manifestations of the same underlying dynamical process. There is an extraordinarily large displacement to higher frequencies in the γ peak from its value in the liquid at 298 K to that in the glass below T_g. Simultaneously the β peak moves from GHz to kHz frequencies. This behaviour is mirrored by other solutes in different glassy environments and by a simple approximation of the Liouville equation of motion for itinerant libration.

[1] See, for example, M. Evans, *Dielectric and Related Molecular Processes*, (Spec. Periodical Report, The Chemical Society, London, 1977), vol. 3, p. 1.
[2] A. R. Davies, G. J. Evans and M. W. Evans, *Adv. Chem. Phys.*, to be published.
[3] A. R. Davies and M. W. Evans, *Mol. Phys.*, 1978, **35**, 857.
[4] G. Williams, *Dielectric and Related Molecular Processes* (Spec. Periodical Report, The Chemical Society, London, 1977), vol. 2.
[5] G. J. Evans and M. W. Evans, *3rd Int. Conf. Submillimetre Waves and their Applications, Infra-red Physics*, (Guildford, 1978).

[6] W. T. Coffey, G. J. Evans, C. J. Reid and M. Evans, *Chem. Phys. Letters*, 1978, **56**, 529 (this letter refers to a concentration of 3 % v/v).

[7] G. P. Johari and M. Goldstein, *J. Chem. Phys.*, 1970, **53**, 2372; 1973, **58**, 1766; G. P. Johari and C. P. Smyth, *J. Chem. Phys.*, 1972, **56**, 4411; G. P. Johari, *J. Chem. Phys.*, 1973, **58**, 1766.

[8] J. H. Calderwood and W. T. Coffey, *Proc. Roy. Soc. A*, 1977, **356**, 269; W. T. Coffey, G. J. Evans, M. W. Evans and G. H. Wegdam, *J.C.S. Faraday II*, 1978, **74**, 310; W. T. Coffey and M. W. Evans, *Mol. Phys.*, 1978, **35**, 975; M. W. Evans, *Mol. Phys.*, 1977, **34**, 963.

[9] C. J. Reid, G. J. Evans and M. W. Evans, *J.C.S. Faraday II*, 1978, **74**, 343.

[10] P. N. Brier and A. Perry, *Adv. Mol. Rel. Int. Proc.*, 1979, in press.

[11] C. C. Bradley, H. A. Gebbie, A. C. Gilby, V. V. Kechin and J. H. King, *Nature*, 1966, **211**, 839.

[12] I. Darmon and C. Brot, *Mol. Cryst.*, 1967, **2**, 301.

[13] H. Mori, *Progr. Theor. Phys.*, 1965, **34**, 399; 1964, **33**, 423.

[14] F. Hermans, E. Kestermont, R. van Loon and R. Finsy, *3rd Int. Conf. Submillimetre Waves and their Applications*, (Guildford, 1978), to be published.

[15] W. T. Coffey, G. J. Evans and M. Evans, *J. Phys. D.*, submitted.

[16] P. S. Damle, A. Sjölander and K. S. Singwi, *Phys. Rev.*, 1968, **165**, 277.

(PAPER 8/1782)